

See discussions, stats, and author profiles for this publication at: <https://www.researchgate.net/publication/228867860>

Solid-State ^{13}C NMR Study of Chiral Twisted Conformation Attributable to Chirality in Smectic Phases of Achiral Banana-Shaped Molecules

ARTICLE in THE JOURNAL OF PHYSICAL CHEMISTRY A · MAY 2004

Impact Factor: 2.69 · DOI: 10.1021/jp031277z

CITATIONS

47

READS

16

9 AUTHORS, INCLUDING:



Hiromichi Kurosu

Nara Women's University

144 PUBLICATIONS 1,713 CITATIONS

SEE PROFILE



Sungmin Kang

Tokyo Institute of Technology

93 PUBLICATIONS 629 CITATIONS

SEE PROFILE



Masato Sone

Tokyo Institute of Technology

138 PUBLICATIONS 1,321 CITATIONS

SEE PROFILE



Hideo Takezoe

Tokyo Institute of Technology

686 PUBLICATIONS 15,126 CITATIONS

SEE PROFILE

Solid-State ^{13}C NMR Study of Chiral Twisted Conformation Attributable to Chirality in Smectic Phases of Achiral Banana-Shaped Molecules

Hiromichi Kurosu, Mami Kawasaki, Mitsuyo Hirose, and Maki Yamada

Department of Textile and Apparel Science, Faculty of Human Life and Environment,
Nara Women's University, Kitauroya Nishimachi, Nara 630-8506, Japan

Sungmin Kang, Jirakorn Thisayukta, Masato Sone, Hideo Takezoe, and Junji Watanabe*

Department of Organic and Polymeric Materials, Tokyo Institute of Technology, Ookayama, Meguro-ku,
Tokyo 152-8552, Japan

Received: November 26, 2003

Solid-state ^{13}C NMR measurements were made for the B2 and B4 phases of the achiral banana-shaped molecule, P-14-O-PIMB, which exhibits a direct transformation from the B2 phase to the B4 phase. In both phases, an NMR resonance signal assigned to carbonyl carbons of the ester linkages appears as doublet peaks, showing that the two carbonyl carbons are circumstanced in different electronic environments on the NMR time scale. The chemical shifts of the two peaks are 165.6 and 163.9 ppm in the B2 phase, and these values are not changed in the transformation to the low-temperature B4 phase. To explain this distinct splitting of the carbonyl carbon signal, we take three assumptions into account: (1) the molecules are accommodated in the unique phase, but the conformational exchange between two states takes place slowly; (2) the two side wings of each molecule experience fast interconformational jumps, but their “average conformer” is different, thus giving two different peaks in the spectra; and (3) the individual molecule claims the twisted conformation, where the two carbonyl carbons of the ester moieties are twisted away from each other by rotating out of the molecular core plane with different dihedral angles. From the present ^{13}C NMR results, the first and second possibilities are ruled out, and it is concluded that the banana-shaped molecules assume the twisted conformation, which is attributable to the origin of the chirality of the B2 and B4 phases in the achiral banana-shaped molecular system.

1. Introduction

The discovery of electro-optic switching by Niori et al.¹ and the suggestion of chirality by Sekine et al.² in a fluid achiral smectic B2 phase formed by bent-shaped P-*n*-O-PIMB homologous molecules motivated the study of polar order and chiral superstructures in achiral liquid crystal molecular systems. In these materials, the macroscopic polarity resulted from C_{2v} symmetry due to a close packing of the bent molecules into a layer.^{3–5} Further interesting is that the molecules in the B2 phase are tilted in the smectic layer, resulting in the layer chirality.^{6,7} The chiral relationship is produced between the layer normal \mathbf{z} , the direction of the molecular tip \mathbf{b} , and the local molecular orientation director \mathbf{n} . The layer chirality is then defined by $\mathbf{b} = (\mathbf{z} \times \mathbf{n})/|\mathbf{z} \times \mathbf{n}|$ and is either (+) or (–), depending respectively on whether the product of $\mathbf{z} \times \mathbf{n}$ points in the direction along \mathbf{b} or $-\mathbf{b}$ (refer to Figure 1 of ref 8). A spontaneous polarization \mathbf{P} arises parallel or antiparallel to \mathbf{b} . Subsequently, a succession of layers defines the polar order (ferroelectric or antiferroelectric) and the overall layer chirality (homochiral or racemic). The term “homochiral” is used to indicate that all layers in a certain domain have layer chirality of the same sign, and the term “racemic” is used to indicate an alternation of the sign of the layer chirality from layer to layer. Allowing synclinic and anticlinic stacking of the tilted polar smectic layers with C_2 symmetry, there are then four possible

arrangements of the polar order and layer chirality, two homochiral SmC_SP_F and SmC_AP_A structures and two racemic SmC_SP_A and SmC_AP_F structures.⁶ The subscripts “S” or “A” added to SmC refer to “synclinic” or “anticlinic” molecular alignments in the smectic layers, and the “F” and “A” subscripts added to P stand for “ferroelectric” and “antiferroelectric” polar orders. This heterogeneity of structures has made it difficult to understand the structure and properties of the B2 phase.^{8–11}

The lowest temperature B4 phase in the P-*n*-O-PIMB homologues also shows a chiral feature.^{2,7,12,13} It is apparently a solid phase, but it differs from a typical crystalline phase. The most interesting feature of this phase is the appearance of a transparent blue color. Subsequently, the B4 phase shows a circular dichroism at about 400 nm. The blue color, hence, is attributed to the selective reflection of left- or right-handed circularly polarized light, suggesting the existence of helical structure. In fact, detailed observation of microscopic textures and circular dichroism indicated the simultaneous existence of two helical domains with opposite optical rotations.^{7,12,13} Since these combined features are recognized only when the sample is prepared from a planarily aligned B2 phase, the helical structure is thought to be formed with the helical axis parallel to the layers, like in the twisted grain boundary (TGB) phase (see Figure 18 of ref 13). The transparency is due to the twisted blocks, with each block smaller than the wavelength of the light. In the B4 phase, the molecules are found not to be tilted toward the layer normal. A mesophase similar to the B4 phase has

* Corresponding author. E-mail: jwatanab@polymer.titech.ac.jp.

recently been observed in some achiral polyphilic bent-core molecules; however, these molecules have additional tilting in the layers.¹⁴ This has led us to consider a different source of chirality from that in the B2 phase. The chirality was argued to be due to a helical twisted conformation characteristic of the particular type of banana-shaped molecules.^{2,13,15} Moreover, Jakli et al.¹⁶ have observed optically active domains with clear boundaries in both antiferroelectric and ferroelectric transformed states in an all-ester banana-shaped molecule. Importantly, they have found that this exhibition of the chiral domain is not due to the layer chirality, but the enantiomorphic property is more likely to be created by the twisted conformation in that molecule.

The simple conclusion deduced from the above results is that both the B2 and B4 phases are intrinsically chiral, but the origin of chirality is apparently different between these two phases. In our recent study,¹⁷ however, we have found that there is a strong correlation of chirality between the B2 and B4 phases. A study was done on the first reported banana-shaped molecule, P-12-O-PIMB, in which the molecule exhibits a direct transition from the B2 phase to the B4 phase enantiotropically. To avoid the complexity of multiple formations of the B2 structures, we prepared each single type of the layer structures of the B2 phase and performed the circular dichroism (CD) measurement for each structure. The results showed the distinct CD peak at around 400 nm for the homochiral SmC_SP_F and SmC_AP_A layer structures, while no CD effect was observed in the racemic layer structure. On the other hand, the B4 phase always showed the CD peak at a similar wavelength, but with opposite sign to the that from B2 phase. By coupling optical microscopy measurements with the CD results, we have further found that even if any layer structure of the B2 phase is initially prepared, it is readily converted to the homochiral SmC_AP_A layer structure on temperature cycling through the lowest temperature B4 phase. This implies that once the chiral domains are formed in the B4 phase, they are conserved thereafter on the succeeding transformation between the B2 and B4 phases. For this conservation of chirality, there should be a common chiral source responsible for the chiral structures of both the B2 and B4 phases. That is a conformational chirality.

The conformational chirality was first proposed on the basis of the ¹³C NMR data, in which the NMR signal due to the carbonyl carbons appears as a doublet for both the B2 and B4 phases.² FT-IR measurements also supported the existence of the chiral conformation.^{18,19} In our previous studies, however, we have not been concerned with the heterogeneity of the structures of the B2 phase. Additionally, the resolution of the NMR spectrometer and the temperature control facilities were not sufficient to obtain qualitative data, especially in the high-temperature B2 phase. In this study, we carefully prepared a single type of each layer structure of the B2 phase and observed the well-defined NMR spectra with an appropriate signal-to-noise ratio. The material used in this work is P-14-O-PIMB, in which the molecule shows the same phase sequence as that of P-12-O-PIMB. Our most important finding is that the carbonyl carbon peak resonates as a doublet signal in either the homochiral SmC_AP_A or racemic SmC_SP_A layer structure of the B2 phase as well as in the B4 phase. Moreover, the chemical shifts are almost constant in both the B2 and B4 phases, suggesting that the molecule assumes similar twisted conformations in these two mesophases.

2. Experimental Section

2.1. Materials. The material used is one of the classic banana-shaped molecules in the P-*n*-O-PIMB homologous series, 1,3-

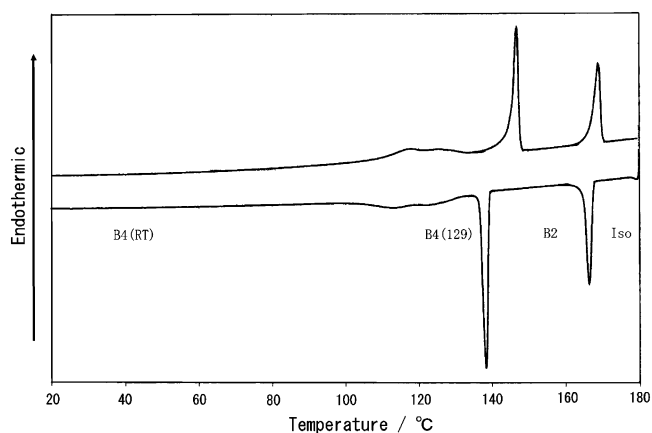
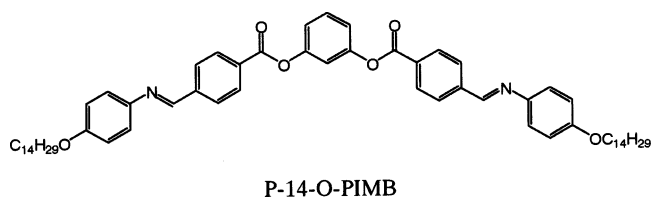


Figure 1. DSC thermograms of P-14-O-PIMB taken on heating and cooling at the rate of 10 °C/min.

phenylene bis[4-((4-(14-tetradecyloxyphenyl)iminomethyl)-benzoate)] (P-14-O-PIMB), as shown below:



The synthesis of this material can be found in ref 2.

2.2. NMR Measurements. ¹³C CP/MAS NMR data are collected by utilizing a JNM EX-270 NMR spectrometer, operating at a frequency of 67.8 MHz with cross-polarization/magic angle spinning (CP/MAS) and variable-temperature (VT) accessories. Sample is placed in a zirconium cylindrical rotor and spun at speeds up to 4.5 kHz. The contact time is 2 ms, and the repetition time is 5 s. The ¹H radio frequency (rf) field strength is about 60 kHz. Spectra are obtained by an accumulation of 1000–2000 scans so as to achieve a reasonable signal-to-noise ratio. At 179 °C, the ¹³C NMR spectrum is measured under the same conditions, except for the pulse sequence and spinning speed. Using MASGHD as the pulse sequence technique, the ¹³C signal is detected by carbon 90° pulse when gated high-power proton decoupling is used and the sample is spun at speeds up to 2.0 kHz. The ¹³C chemical shifts (δ) are calibrated indirectly with adamantane as the external standard (29.5 ppm relative to tetramethylsilane). The solution-state ¹³C NMR spectrum is measured using a JNM GSX-500 NMR spectrometer operating at a frequency of 75.5 MHz.

3. Results

3.1. Thermotropic Behavior of P-14-O-PIMB. Figure 1 shows the DSC thermogram of P-14-O-PIMB. Two sharp peaks and one broad peak are observed in both the heating and cooling curves, as shown in Figure 1. The two sharp peaks at 166 and 138 °C on the cooling trace correspond to the isotropic–B2 and B2–B4 phase transitions, respectively. Because of the additional broad peak at around 120 °C, just below the B2–B4 transition, which may be due to an internal complex transformation of the B4 phase itself, we designate the B4 phases at room temperature and 129 °C as B4(RT) and B4(129), respectively.

3.2. High-Resolution Solid-State ¹³C NMR Spectra. Figure 2 depicts the solid-state VT ¹³C NMR stack spectra of P-14-O-PIMB measured in the isotropic, B2, and B4 phases. For the isotropic phase at 179 °C, the solid-state NMR spectrum is obtained by using the MASGHD pulse sequence technique,

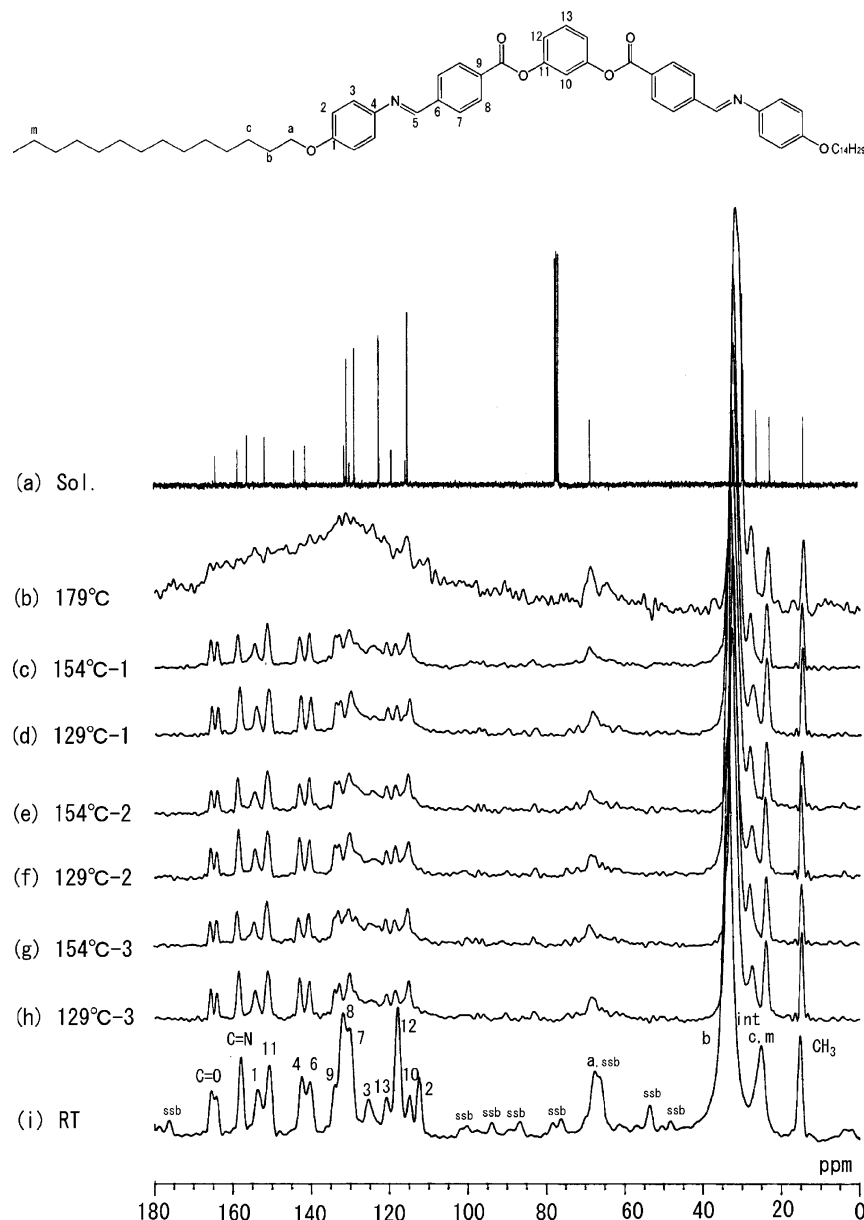


Figure 2. ^{13}C NMR spectra for P-14-O-PIMB: (a) solution state; (b) isotropic melt at 179 $^{\circ}\text{C}$ (MASGHD method); (c, e, and g) B2(154) phase (CP/MAS method) at 154 $^{\circ}\text{C}$; (d, f, and h) B4(129) phase (CP/MAS method) at 129 $^{\circ}\text{C}$; (i) B2(RT) phase at room temperature (CP/MAS method). The spinning sidebands are indicated with “ssb”.

which detects the ^{13}C signal by carbon 90° pulse. The other NMR spectra for the B2 and B4 phases are obtained by CP/MAS method. For reference, the solution-state NMR spectrum is also shown in Figure 2a. All the peaks are well interpreted, as displayed in Figure 2. The peaks of the carbonyl carbons of the ester moieties linking the central core and two side wings are observed around 164 ppm. The peaks around 158, 110–155, and 10–70 ppm are assigned to the carbon atoms of the Schiff base group ($\text{C}=\text{N}$), aromatic rings, and aliphatic chains, respectively.²⁰

Solid-state NMR measurements are performed in a series of steps. First, the sample is heated to 179 $^{\circ}\text{C}$ to obtain the NMR data on the isotropic melt (Figure 2b). The sample is then slowly cooled to 154 $^{\circ}\text{C}$, and then to 129 $^{\circ}\text{C}$, to collect the NMR data on the B2 and B4 phases (Figure 2c,d). After the fundamental measurements for the three phases, we once again cycle the temperature of the probe between 154 (B2(154)) and 129 $^{\circ}\text{C}$ (B4(129)) and take measurements twice at each temperature (see Figure 2e–h). Finally, the measurement is carried out in the B4 phase at room temperature, as shown in Figure 2i. In Figure

3, the spectra are zoomed in the chemical shift range from 150 to 170 ppm. The bar spectra of the chemical shifts that belong to the carbon atoms of the ester moiety, Schiff base, and alkyl-terminal tails are illustrated in Figure 4.

4. Discussion

The most important point in this work is related to the signals from the carbonyl carbons of the ester linkages located between the two side wings and the central core. As can be seen in Figure 2b, the peaks of aromatic carbons at the central core are broadened, so there is no resonance peak detected in the isotropic state. This can be understood on the basis of the reduced efficiency of the proton decoupling (the decoupling field is about 60 kHz for this experiment) and/or interference between motional and magic angle sample spinning frequencies (2 kHz for this experiment), which cause significant broadening of the line width. On cooling to the B2 phase, the signal at $\delta \sim 165$ ppm appears as a doublet (see Figure 3). A similar doublet peak is also observed in the B4(129) phase. The chemical shifts of

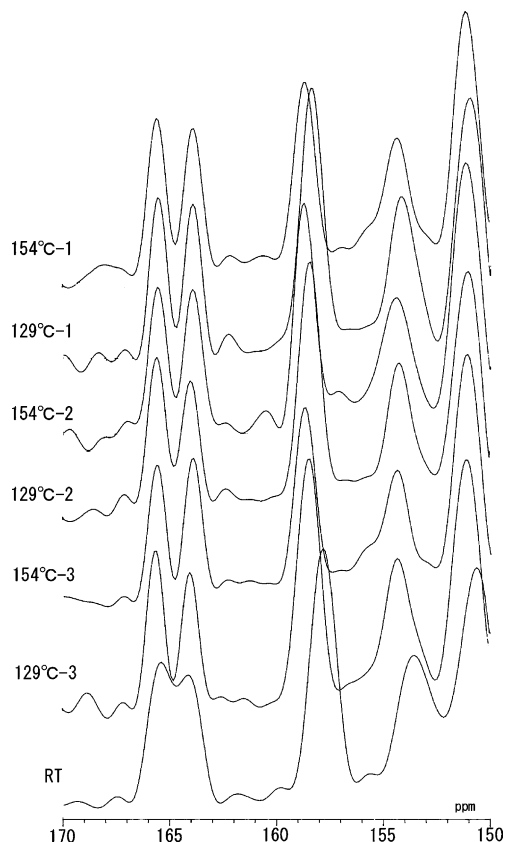


Figure 3. Expanded ^{13}C CP/MAS NMR spectra of P-14-O-PIMB.

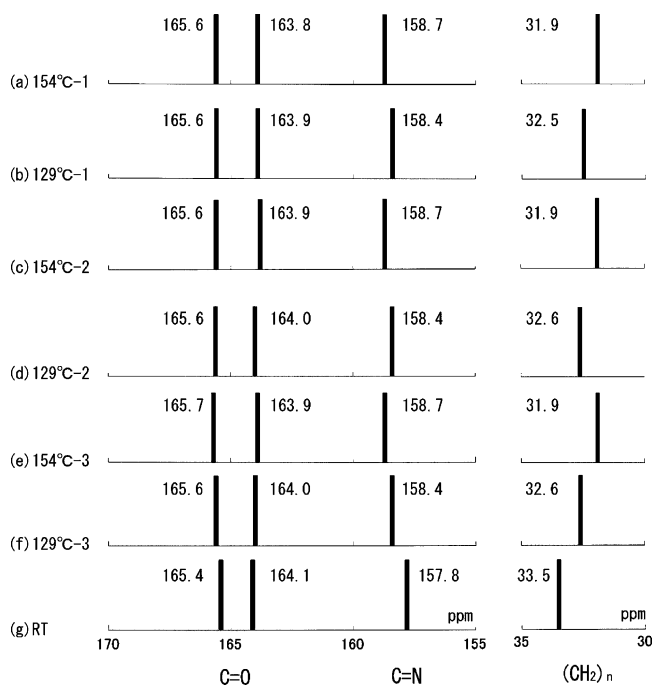


Figure 4. Schematic diagram for peak positions of carbonyl carbon, C=N, and alkyl carbon in the ^{13}C CP/MAS NMR spectra of P-14-O-PIMB.

the doublet peaks are almost constant at 165.6 and 163.8 ppm for both the B2(154) and B4(129) phases, as illustrated schematically in Figure 4.

Since the molecular motion in the fluid liquid crystal is relatively high enough to average the electronic field around the carbons, the NMR signal should principally appear as a singlet as observed in the solution state. Hence, it is unusual that the doublet peak is observed, even in the B2 phase, in which

the molecules are supposed to pack laterally with a liquid-like nature, similar to that in the conventional SmA or SmC. Further, it is also nontrivial that such a doublet signal is observed only for the carbonyl carbons.

The splitting of the signal obviously indicates that the carbonyl carbons are situated under different electronic environments on the NMR time scale. To account for this hypothesis, we first envisage that there should be at least two situations that force the molecules to take up different conformations. In fact, this is possible because the tilted polar smectic layers with C_2 symmetry allow the formation of the two homochiral (SmC_AP_A and SmC_SP_F) and two racemic (SmC_SP_A and SmC_AP_F) layer structures in the B2 phase.⁶ In the most recent study,¹⁷ we have found that the racemic SmC_AP_F structures are formed dominantly on cooling from the isotropic melt, but on cycling heating and cooling between the B2 and B4 phases, only the homochiral SmC_AP_A layer structure exists. To understand whether this heterogeneous formation of the layer structures might be related to the splitting of the signal of the carbonyl carbon, we carried out the NMR measurement for the B2 phase prepared by the same experimental procedure described above. As can be seen in Figure 3, the signals are not affected at all by temperature cycling between the B2 and B4 phases, showing that the doublet signal is essentially observed irrespective of the type of the layer structures of the B2 phase.

Thus, we reach the conclusion that the splitting of the signal from the carbonyl carbons is attributed to the intrinsic molecular conformation, which is independent of the type of B2 layer structure. Three possible assumptions are, therefore, considered in the following:

- (1) The carbonyl carbons of the molecule undergo slow exchange dynamically between two states.
- (2) The two wings of each molecule experience fast interconformational jumps, but their "average conformer" is different, thus giving two different peaks in the spectra.
- (3) The carbonyl carbons in the individual molecule make different angles with respect to the central phenyl ring, i.e., twisted conformation and/or chiral conformation.

To investigate the molecular motion, we use the spinning sideband technique. From a comparison of spectra b and c to spectrum i in Figure 2, we know that the CP/MAS spectra at 154 and 129 °C show negligible spinning sidebands, although they are clearly recognized at room temperature. This means that the molecular motion partially averages the chemical shift anisotropy at these high temperatures. Furthermore, one can see that the chemical shift difference of the doublet signal is almost constant on cooling from 154 to 129 °C, though it becomes slightly narrower at room temperature. This maintenance of the chemical shift difference does not fulfill but rather eliminates the first assumption, since the chemical shift difference should increase with decreasing temperature if the molecules undergo exchange between two states.

Under the second assumption, if the two side wings of each molecule experienced "fast interconformational jumps", the chemical shifts of the carbonyl carbons measured at 129 °C and room temperature should be unchanged because a moderate reduction of the frequency for the interconformational jumps does not affect the chemical shift. However, if a strong reduction of the frequency for the interconformational jumps occurred, four peaks for the carbonyl carbons should be observed. Nevertheless, the chemical signals of the carbonyl carbon at 129 °C are shifted as compared with that of the carbonyl carbon at room temperature, and the chemical shift difference becomes slightly narrower at room temperature. This implies that the

observation of the change of the chemical shift rules out the second assumption.

At this stage, the third assumption, whereby the molecule minimizes its energy by twisting the carbonyl carbons out of the molecular plane, becomes our primary focus. MO calculation of the conformational energy around the two ester bonds in the P-*n*-O-PIMB homologues shows that the twisted conformations with right- and left-handed senses essentially exist among four possible conformations.¹⁵

As the twisted arrangement of the two side wings is like a screw propeller, this can cause the split signals for the carbonyl carbons. However, it is basically thought that the molecules in the fluid B2 phase are mobile, so as to have conformational freedom as well as rotational freedom to some extent. Hence, the molecules should not keep up the certain twisted conformation; after a prolonged time, the twisted conformation with a certain helical sense would be converted to that with the other helical sense or other conformations. In fact, the potential energy barriers between the four possible conformations are about 0.5 kcal/mol, which is smaller than the thermal energy in the high-temperature range of the B2 phase. In the B2 phase, however, the conformational chirality should be closely coupled with the layer chirality induced by molecular tilting.¹⁷ In other words, the conformational chirality enables the molecules to tilt in a certain direction, such that the left-handed conformation induces the tilting of molecules to the left side, while the right-handed one causes tilting to the right. Accordingly, the alternation of the conformational chirality should be followed by an alternation of the tilt direction in the layer, which is supposed to have a somewhat high-energy barrier. This may be a reason the helical conformation is thermodynamically sustained in the B2 phase.

It can be seen that the chemical shifts of the carbonyl carbons are not significantly changed upon the transformation between the B2(154) and B4(129) phases. This indicates that there is no large difference in the torsion angles between the carbonyl carbons and the central core of the molecule in both the B2 and B4(129) phases. The present result is consistent with and strongly supports our recent finding that the conformational chirality is conserved on the transformation between the two phases.¹⁷

The chemical shifts of the carbon atom of the Schiff base unit (C=N) on the side wings and methylene carbons (—CH₂—) on the alkyl-terminal tails apparently depend on the structure of the mesophases, as can be seen in Figure 4. The chemical shifts of the C=N carbon are 158.7 and 158.4 ppm for the B2 and B4 phases, respectively. From the previous studies, we have learned that in the B2 phase the molecules are tilted by 35° to the layer normal, while they lie perpendicular to the layer in the B4 phase. We believe that this difference in the molecular orientations crucially affects the chemical shift of the C=N carbon.²¹

The chemical shifts of the methylene carbons of the B2(154), B4(129), and B4(RT) are 31.9, 32.6, and 33.5 ppm, respectively. These values range between the values of trans zigzag conformation and the amorphous state, showing a rapid exchange of the trans and gauche conformers. The lower-field shift of the peak means there is a higher fraction of the trans conformers.²² The time-averaged fractions of the trans conformers are estimated as 0.78, 0.85, and 0.93 for the B2(154), B4(129), and B4(RT) phases, respectively.

5. Conclusion

Solid-state ¹³C NMR spectroscopy, with a well-defined signal-to-noise ratio, was successfully carried out for the B2 and B4 phases of the classic banana-shaped molecule "P-14-O-PIMB". The NMR signal of the carbonyl carbons appears as a doublet pattern in both the B2 and B4 phases, showing that there are two different electronic circumstances around the carbonyl carbons on the NMR time scale. The chemical shifts of the two signals are 165.6 and 163.9 ppm for the B2 phase, and these values remain almost constant through the transformation to the B4 phase. The distinct split pattern appears to be related to the twisted conformation of a constituent banana-shaped molecule in which the two carbonyl carbons of the ester linkages orient with different dihedral angles relative to the central core. It is important to note that the chemical shifts are not varied by temperature cycling between the B2 and B4 phases. Thus, similar twisted conformations are well preserved in both phases, strongly suggesting that the twisted conformation is the origin of chirality in the B2 and B4 phases.

References and Notes

- (1) Niori, T.; Sekine, T.; Watanabe, J.; Takezoe, H. *J. Mater. Chem.* **1996**, *6*, 1231.
- (2) Sekine, T.; Niori, T.; Sone, M.; Watanabe, J.; Choi, S.; Takanishi, Y.; Takezoe, H. *Jpn. J. Appl. Phys.* **1997**, *36*, 6455.
- (3) Watanabe, J.; Shimizu, K.; Nakata, Y. *J. Phys. II (France)* **1994**, *4*, 581.
- (4) Watanabe, J.; Niori, T.; Choi, S. W.; Takanishi, Y.; Takezoe, H. *Jpn. J. Appl. Phys.* **1998**, *37*, L401.
- (5) Watanabe, J.; Izumi, T.; Niori, T.; Zen-nyoji, M.; Takanishi, Y.; Takezoe, H. *Mol. Cryst. Liq. Cryst.* **2000**, *346*, 77.
- (6) Link, D. R.; Natale, G.; Shao, R.; MacLennan, J. E.; Clark, N. A.; Korblova, E.; Walba, D. M. *Science* **1997**, *278*, 1924.
- (7) Heppke, G.; Moro, D. *Science* **1998**, *279*, 1872.
- (8) Nakata, M.; Link, D. R.; Thisayukta, J.; Takanishi, Y.; Ishikawa, K.; Watanabe, J.; Takezoe, H. *J. Mater. Chem.* **2001**, *11*, 2694.
- (9) Thisayukta, J.; Niwano, H.; Takezoe, H.; Watanabe, J. *J. Mater. Chem.* **2001**, *11*, 2717.
- (10) Zen-nyoji, M.; Takanishi, Y.; Ishikawa, K.; Thisayukta, J.; Watanabe, J.; Takezoe, H. *J. Mater. Chem.* **1999**, *9*, 2775.
- (11) Shen, D.; Pegenau, A.; Diele, S.; Wirt, I.; Tchierske, C. *J. Am. Chem. Soc.* **2000**, *122*, 1593.
- (12) Thisayukta, J.; Nakayama, Y.; Kawauchi, S.; Takezoe, H.; Watanabe, J. *J. Am. Chem. Soc.* **2000**, *122*, 7441.
- (13) Thisayukta, J.; Takezoe, H.; Watanabe, J. *Jpn. J. Appl. Phys.* **2001**, *40*, 3277.
- (14) Dantlgraber, G.; Eremin, A.; Diele, S.; Hauser, A.; Kresse, H.; Pelzl, G.; Tschierske, C. *Angew. Chem.* **2002**, *41*, 2408.
- (15) Imase, T.; Kawauchi, S.; Watanabe, J. *J. Mol. Struct.* **2001**, *560*, 275.
- (16) Jakli, A.; Huang, Y.-M.; Fodor-Csorba, F.; Vajda, A.; Galli, G.; Diele, S.; Pelzl, G. *Adv. Mater.* **2003**, *15*(19), 1606.
- (17) Niwano, H.; Nakata, M.; Thisayukta, J.; Link, D. R.; Takezoe, H.; Watanabe, J. To be published.
- (18) Zen-nyoji, M.; Takanishi, Y.; Ishikawa, K.; Thisayukta, J.; Watanabe, J.; Takezoe, H. *Mol. Cryst. Liq. Cryst.* **2001**, *366*, 693.
- (19) Gorecka, E.; Nakata, M.; Mieczkowski, J.; Takanishi, Y.; Ishikawa, K.; Watanabe, J.; Takezoe, H.; Eichhorn, S. H.; Swager, T. M. *Phys. Rev. Lett.* **2000**, *85*, 2526.
- (20) Sone, M.; Harkness, B. R.; Kurosu, H.; Ando, I.; Watanabe, J. *Macromolecules* **1994**, *27*, 2776.
- (21) Kurosu, H.; Ookubo, T.; Tuchiya, H.; Ando, I.; Watanabe, J. *J. Mol. Struct. (THEOCHEM)* **2001**, *574*, 153.
- (22) Ishikawa, S.; Kurosu, H.; Ando, I. *J. Mol. Struct.* **1990**, *248*, 361.